Inversion of the X-ray transform from limited angle parallel beam region of interest data with applications to electron tomography

Ozan Öktem[*1] and **Eric Todd Quinto**[**2]

[1] Sidec, Torshamnsgatan 28A, SE-164 40 Kista, Sweden
[2] Department of Mathematics, Tufts University, 503 Boston Avenue, Medford, MA 02155, USA

We present a new local tomographic algorithm applicable to electron microscopy tomography. Our algorithm applies to the standard data acquisition method, single-axis tilting, as well as for more arbitrary acquisition methods. Using microlocal analysis we put the reconstructions in a mathematical context, explaining which singularities are stably visible from the limited data given by the data collection protocol in the electron microscope.

1 Introduction to electron tomography

The problem of recovering the three-dimensional structure of an individual molecule (*e.g.* a protein or a macromolecular assembly) in its natural environment at highest possible resolution plays a central role in understanding biological processes in time and space. The publication of [1] in 1968 marked the beginning of *electron tomography (ET)* where the idea of recovering the structure of a sample from *transmission electron microscope (TEM)* data using principles of tomography was first outlined. ET is currently the *only* approach that allows one to reconstruct the three-dimensional structure of *individual* molecules in the cellular (*in-situ*) or aqueous (*in-vitro*) environment. Since the ability to study individual molecules is important in order to address many biological problems, ET is nowadays enjoying an increasing interest within life sciences.

A specimen that is to be imaged in a TEM must first be physically immobilized since it is imaged in vacuum. It also needs to be thin (about 70–100 nm) if enough electrons are to pass through to form an image. The purpose of sample preparation is to achieve this *without interfering with the structure of the specimen*. Data collection in ET is done by mounting the specimen on a holder (goniometer) that allows one to change its positioning relative to the optical axis of the TEM. For a fixed position, the specimen is radiated with an electron beam and the resulting data, referred to as a *micrograph*, is recorded by a detector. The most common data acquisition geometry is *single axis tilting* where the specimen plane is only allowed to rotate around a fixed single axis, called the *tilt axis*, which is orthogonal to the optical axis of the TEM. The rotation angle is called the *tilt angle* and its angular range is usually contained in a subset of $[-60^\circ, 60^\circ]$. Since the specimen extends far beyond the area exposed to the electrons, we are dealing with region of interest tomographic data.

Under appropriate approximations and transformations [2, 3, 4], the measured data can be thought of as representing line integrals of a function, which we choose to call the *scattering potential*, related to the scattering properties of the specimen which in turn provides the molecular structure of the specimen. In particular, when ET data is collected according to the single axis tilting scheme, the corresponding reconstruction problem can be recast as the problem of inverting the X-ray transform from parallel beam region of interest data with directions on a curve. Again, because of the size of the whole specimen, one can only rotate it in a limited range of angles, so the reconstruction problem is a *limited angle* problem. The region of interest and limited angle issues imply that one has *non-uniqueness* and *severe ill-posedness*. The former means that one cannot exactly reconstruct the scattering potential of the specimen even in cases when one assumes exact data (no measurement errors) and disregards the discretization of the set of lines (*i.e.* one deals with the corresponding continuous problem where data are given over a continuous set of lines). Furthermore, ET data are very noisy, in particular because of the dose problem–the dose needed to get low-noise data destroys the specimen.

2 Λ-tomography

The above mentioned issues arising in ET, namely non-uniqueness and ill-posedness combined with noisy data, point to using a reconstruction method that regularizes by reconstructing only some information about the specimen that can be stably retrieved, in our case, the shape of the boundaries of the molecules in the specimen. Our method is a generalization of Λ-tomography [5, 6]. Limited data Λ-tomography in $\mathbb{R}^2$ has been investigated in [7, 8]. For line complexes in $\mathbb{R}^3$, the cone beam setting has been studied by Louis and Maass [9], Katsevich [10], Anastasio, *et. al.*, [11], and Yee, *et. al.*, [12]. Our work presented here deals with studying Λ-tomography in the limited angle parallel beam setting in $\mathbb{R}^3$.

* Corresponding author: e-mail: ozan.oktem@sidec.com, Phone: +46 8 47 77 614, Fax: +46 8 47 77 601

** This work was supported by the National Science Foundation under grants DMS-0200788 and DMS-0456858 and support from the Wenner Gren Center, Tufts University FRAC, the Humboldt Stiftung, and Sidec Technologies.

For a fixed smooth curve $S \subset S^2$ we define the *parallel beam 3D line complex* $\mathcal{M}_S$ as the manifold of lines parallel to a direction in S. Now, lines in $\mathbb{R}^3$ are uniquely determined by the pair $(\boldsymbol{\omega}, \boldsymbol{x})$ where $\boldsymbol{\omega} \in S^2$ is the direction of the line and $\boldsymbol{x} \in \boldsymbol{\omega}^\perp$ is a point through which the line passes. The Λ-reconstruction operator for inverting the X-ray transform given data on $\mathcal{M}_S$ reads as

$$\mathcal{L}(F) := \mathcal{P}_S^*\big((\mu - \mathcal{D}_S^2)\mathcal{P}(F)\big)$$

where $\mathcal{P}(F)$ is the X-ray transform of to function F that is of interest, which in ET is the scattering potential providing the molecular structure of the specimen. $\mathcal{P}_S^*$ is the corresponding backprojection operator and $\mathcal{D}_S^2$ is a second order differentiation along a consistently chosen tangential direction to the curve S, *i.e.* for a function g defined on $\mathcal{M}_S$ we have

$$\mathcal{P}_S^*(g)(\boldsymbol{x}) := \int_{\boldsymbol{\omega}\in S} g\big(\boldsymbol{\omega}, \boldsymbol{x} - (\boldsymbol{x}\cdot\boldsymbol{\omega})\boldsymbol{\omega}\big)\, d\boldsymbol{\omega} \quad \text{where } \boldsymbol{x} \in \boldsymbol{\omega}^\perp,$$

$$\mathcal{D}_S^2 g\big(\boldsymbol{\omega}, \boldsymbol{x}\big) := \frac{d^2}{ds^2} g\big(\boldsymbol{\omega}, \boldsymbol{x} + s\boldsymbol{\sigma}\big)\Big|_{s=0} \quad \text{where } \boldsymbol{x} \in \boldsymbol{\omega}^\perp \text{ and } \boldsymbol{\sigma} \text{ is the unit tangent to } S \text{ at } \boldsymbol{\omega} \in S.$$

Using microlocal analysis we relate the wave front sets of $\mathcal{L}(F)$, F and $\mathcal{P}(F)$ and characterize those singularities of F that are visible [3]. For example, assume F is smooth except for a jump discontinuity along a smooth hypersurface Γ. Then, a singularity at $\boldsymbol{x} \in \Gamma$ is stably recoverable if and only if there is a line in the line complex $\mathcal{M}_S$ that goes through $\boldsymbol{x}$, is tangent to Γ, and not "bad" (*i.e.* normal to S along the line). In single axis tilting, the "bad" directions are $\boldsymbol{\xi} = (\pm 1, 0, 0)$, *i.e.* jump singularities with normal directions $(-1, 0, 0)$ and $(1, 0, 0)$ could be invisible or could create added streaks [3].

We conclude by showing an example in Figure 1 of Λ-tomography applied to real ET data from an *in-situ* sample.

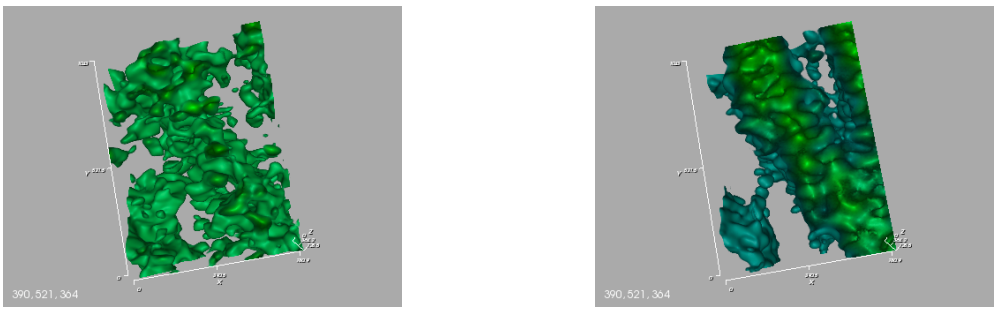

Fig. 1 Volume rendered reconstructions of an *in-situ* tissue sample (could be human, rat or mice kidney). The background noise is suppressed in the Lambda reconstruction to the right and the "V" shaped region containing the slit diaphragm is more clearly defined when compared to the filtered backprojection reconstruction with additional low-pass (10nm-resolution) post-filtering to the left. The ET data was collected from single axis tilting with uniform sampling of the tilt angle in $[-60^\circ, 60^\circ]$ with a 2° step. The pixel size is 0.5241nm and the total dose is $1520\mathrm{e}^-/\mathrm{nm}^2$. A detailed account on the experimental setting and the study objective is given in [13].

Acknowledgements The authors are indebted to Prof. Ulf Skoglund for invaluable help, support, and knowledge as well as for generous access to data sets. The authors thank Prof. Jan Boman of Stockholm University for extremely valuable comments that clarified and refined the microlocal analysis in the article. Finally, we thank Dr. Hans Rullgård of Stockholm University for carefully reading the manuscript. The second author also thanks Prof. Dr. Alfred Louis and Universität des Saarlandes and Prof. Dr. Andreas Rieder and Universität Karlsruhe for their hospitality while this was being researched and written.

References

[1] D. J. De Rosier and A. Klug, Nature **217**, 130–134 (1968).
[2] D. Fanelli and O. Öktem, Electron tomography: A short overview with an emphasis on the absorption potential model for the forward problem., Submitted to Inverse Problems, 2007.
[3] E. T. Quinto and O. Öktem, Local tomography in electron microscopy, Submitted to SIAM Journal of Applied Mathematics, 2007.
[4] P. W. Hawkes and E. Kasper, Principles of Electron Optics. Volume 3. Wave Optics. (Academic Press, 1994).
[5] A. Faridani, E. L. Ritman, and K. T. Smith, SIAM Journal on Applied Mathematics **52**, 459–484 (1992).
[6] E. I. Vainberg, I. A. Kazak, and V. P. Kurozaev, Soviet Journal of Nondestructive Testing **17**, 415–423 (1981).
[7] P. Kuchment, K. Lancaster, and L. Mogilevskaya, Inverse Problems **11**, 571–589 (1995).
[8] E. T. Quinto, Journal of Computational and Applied Mathematics **199**, 141–148 (2006).
[9] A. K. Louis and P. Maaß, IEEE Transactions in Medical Imaging **12**(4), 764–769 (1993).
[10] A. I. Katsevich, Inverse Problems **22**, 627–643 (2006).
[11] M. A. Anastasio, Y. Zou, E. Y. Sudley, and X. Pan, Local cone-beam tomography image reconstruction on chords, Tech. rep., Illinois Institute of Technology, 2006.
[12] Y. Ye, H. Yu, and G. Wang, Inverse Problems **23**, 203–215 (2007).
[13] J. Wartiovaara, L. G. Öfverstedt, J. Khoshnoodi, J. Zhang, E. Makela, S. Sandin, V. Ruotsalainen, R. H. Cheng, H. Jalanko, U. Skoglund, and K. Tryggvason, Journal of Clinical Investigation **114**, 1475–1483 (2004).